Dissipation in circuit quantum electrodynamics:
lasing and cooling of a low-frequency oscillator

Julian Hauss[1,2], Arkady Fedorov[1,3], Stephan André[1], Valentina Brosco[1], Carsten Hutter[1,4],
Robin Kothari[1,5], Sunil Yeshwanth[1,6], Alexander Shnirman[1,7], and Gerd Schön[1]

[1] *Institut für Theoretische Festkörperphysik and DFG-Center for Functional Nanostructures (CFN),*
Universität Karlsruhe, D-76128 Karlsruhe, Germany
[2] *Lichttechnisches Institut, Universität Karlsruhe, D-76128 Karlsruhe, Germany*
[3] *Kavli Institute of Nanoscience, Delft University of Technology, 2600 GA Delft, The Netherlands*
[4] *Department of Physics, Stockholm University, AlbaNova University Center, SE - 106 91 Stockholm, Sweden*
[5] *Department of Physics, Indian Institute of Technology Bombay, Mumbai 400076, India*
[6] *Department of Physics, Indian Institute of Technology, Kanpur 208016, India and*
[7] *Institut für Theorie der Kondensierten Materie,*
Universität Karlsruhe, D-76128 Karlsruhe, Germany

Superconducting qubits coupled to electric or nanomechanical resonators display effects previously studied in quantum electrodynamics (QED) and extensions thereof. Here we study a driven qubit coupled to a low-frequency tank circuit with particular emphasis on the role of dissipation. When the qubit is driven to perform Rabi oscillations, with Rabi frequency in resonance with the oscillator, the latter can be driven far from equilibrium. Blue detuned driving leads to a population inversion in the qubit and lasing behavior of the oscillator ("single-atom laser"). For red detuning the qubit cools the oscillator. This behavior persists at the symmetry point where the qubit-oscillator coupling is quadratic and decoherence effects are minimized. Here the system realizes a "single-atom-two-photon laser".

INTRODUCTION

Recent experiments on quantum state engineering with superconducting circuits realized concepts originally introduced in the field of quantum optics, as well as extensions thereof, e.g., to the regime of strong coupling [1, 2, 3, 4, 5, 6, 7, 8], and prompted substantial theoretical activities [9, 10, 11, 12, 13, 14, 15, 16, 17, 18, 19]. Josephson qubits play the role of two-level atoms while electric or nanomechanical oscillators play the role of the quantized radiation field. In most QED or circuit QED experiments the atom or qubit transition frequency is near resonance with the oscillator. In contrast, in the experiments of Refs. [1], with setup shown in Fig. 1a), the qubit is coupled to a slow LC oscillator with frequency ($\omega_T/2\pi \sim$ MHz) much lower than the qubit's level splitting ($\Delta E/2\pi\hbar \sim 10$ GHz). The idea of this experiment is to drive the qubit to perform Rabi oscillations with Rabi frequency in resonance with the oscillator, $\Omega_R \approx \omega_T$. In this situation the qubit should drive the oscillator and increase its oscillation amplitude. When the qubit driving frequency is blue detuned, the driving creates a population inversion of the qubit, and the system exhibits lasing behavior ("single-atom laser"); for red detuning the qubit cools the oscillator [18]. A similar strategy for cooling of a nanomechanical resonator via a Cooper pair box qubit has been recently suggested in Ref. [20]. The analysis of the driven circuit QED system shows that these properties depend strongly on relaxation and decoherence effects in the qubit.

In the experiments of Ref. [1] an enhancement of the oscillator due to the driving was observed. However, first
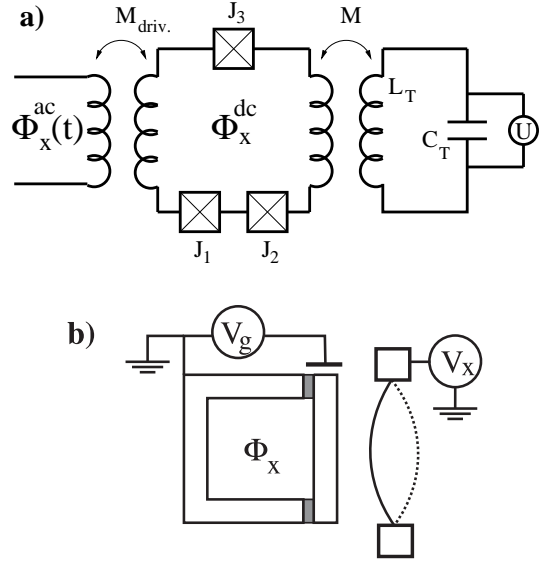

FIG. 1: a) In the setup of Ref. [1] an externally driven three-junction flux qubit is coupled inductively to an LC oscillator. b) A charge qubit is coupled to a mechanical resonator.

attempts to explain the effect theoretically did not resolve several issues [21, 22]. In the experiments, in order to minimize decoherence effects, the Josephson flux qubit was biased near the flux degeneracy point. At this symmetry point also the coupling to the oscillator is tuned to zero, and the enhancement should vanish. Uncontrolled small deviations from the symmetry point might lead to the observed effect [1, 21], but this explanation has not been supported by experiments. Here we explore

an alternative, namely that a quadratic coupling to the oscillator near the resonance condition $\Omega_R \approx 2\omega_T$ is responsible for the observed enhancement. In the following we will consider both linear as well as quadratic coupling, which dominate away from the symmetry point and at this point, respectively. The second unresolved problem is the magnitude of the effect. The experiments [1] showed an increase by a factor $4-5$ in the amplitude, i.e., $16-25$ in the number of oscillator quanta. The theory of Ref. [21], valid in the perturbative regime, predicts a much weaker effect. We obtain a strong effect as follows [18]: due to a detuning of the qubit driving a population inversion is created at the Rabi frequency, and the system becomes a "single-atom laser" at the resonance $\Omega_R \approx \omega_T$, or a "single-atom-two-photon laser" for $\Omega_R \approx 2\omega_T$ [23, 24]. In both cases the lasing threshold is reached for realistic system parameters, and the number of quanta in the oscillator is increased considerably.

A related situation, called "dressed-state lasing", had been studied before in quantum optics [25, 26]. The present scenario differs from that one in so far as the resonator modes are coupled to the low-frequency Rabi oscillations rather than to the high-frequency Mollow transitions. The Rabi frequency can be readily tuned to resonance with the oscillator, which should facilitate reaching the lasing threshold and a proper lasing state. A similar idea has been explored in Ref. [27] in connection with coupling of atoms.

In experiments with the same setup as shown in Fig. 1a) but in a different parameter regime the mechanisms of Sisyphus cooling and amplification has recently been demonstrated [7]. Due to the resonant high-frequency driving of the qubit, depending on the detuning, the oscillator is either cooled or amplified with a tendency towards lasing. The Sisyphus mechanism is most efficient when the relaxation rate of the qubit is close to the oscillator's frequency. In contrast, in the present paper we concentrate on the "resolved sub-band" regime where the dissipative transition rates of the qubits are much lower than the oscillator's frequency.

Also in situations where the qubit, e.g., a Josephson charge qubit, is coupled to a nano-mechanical oscillator (Fig. 1b) it either cools or amplifies the oscillator. On one hand, this may constitute an important tool on the way to ground state cooling. On the other hand, this setup provides a realization of what is called a SASER [28].

Lasing and cooling of the oscillator has also been observed in a slightly different setup, when the ac-driven qubit is replaced by a driven superconducting single-electron transistor biased near the Josephson quasiparticle cycle [29, 30, 31]. When the SSET is coupled to a nanomechanical or electric oscillator it can be used to either cool the oscillator [32, 33, 34, 35, 36, 37] or to produce laser-like behavior. The latter has recently been observed in experiments [38].

THE SYSTEM

The Hamiltonian

The systems to be considered are shown in Fig. 1. A qubit is coupled to an oscillator and driven to perform Rabi oscillations. To be specific we first analyze the flux qubit coupled to an electric oscillator (Fig. 1a) with Hamiltonian

$$
\begin{aligned}
H \;=\; & -\frac{1}{2}\,\epsilon\left(\Phi_x^{dc}\right)\sigma_z - \frac{1}{2}\,\Delta\sigma_x - \hbar\Omega_{R0}\cos(\omega_d t)\,\sigma_z \\
& + \hbar\omega_T\,a^\dagger a \;+\; g\,\sigma_z\left(a + a^\dagger\right)\;.
\end{aligned} \tag{1}
$$

The first two terms describe the qubit, with Pauli matrices $\sigma_{x,z}$ operating in the flux basis of the qubit. The energy bias between the flux states $\epsilon(\Phi_x^{dc})$ is controlled by an external DC magnetic flux, and Δ is the tunneling amplitude between the basis states. The resulting level spacing $\Delta E \equiv \sqrt{\epsilon^2 + \Delta^2}$ typically lies in the range of several GHz. The third term accounts for the driving of the qubit by an applied AC magnetic flux with amplitude Ω_{R0} and frequency ω_d. The last two terms describe the oscillator with frequency $\omega_T = 1/\sqrt{L_T C_T}$, which for the experiments of of Ref. [1] lies in the range of several 10 MHz, as well as the qubit-oscillator interaction. We estimate the coupling constant $g \approx M I_p I_{T,0}$ to be of the order of 10 MHz. Here M is the mutual inductance, I_p the magnitude of the persistent current in the qubit, and $I_{T,0} = \sqrt{\hbar\omega_T/2L_T}$ the amplitude of the vacuum fluctuation of the current in the LC oscillator.

After transformation to the eigenbasis of the qubit, which is the natural basis for the description of the dissipation, the Hamiltonian reads

$$
\begin{aligned}
H \;=\; & -\frac{1}{2}\,\Delta E\,\sigma_z - \hbar\Omega_{R0}\cos\left(\omega_d t\right)\left(\sin\zeta\,\sigma_z - \cos\zeta\,\sigma_x\right) \\
& + \hbar\omega_T\,a^\dagger a + g\left(\sin\zeta\,\sigma_z - \cos\zeta\,\sigma_x\right)\left(a + a^\dagger\right)\;,
\end{aligned} \tag{2}
$$

with $\tan\zeta = \epsilon/\Delta$ and $\Delta E \equiv \sqrt{\epsilon^2 + \Delta^2}$.

Because of the large difference of the energy scales between the qubit and the oscillator, $\Delta E \gg \hbar\omega_T$, it is tempting, in the spirit of the usual rotating wave approximation (RWA), to drop the transverse coupling term $-g\cos\zeta\,\sigma_x\left(a + a^\dagger\right)$ of Eq. (2). However, near the symmetry point (where $\sin\zeta = 0$) the longitudinal coupling is weak. Therefore, we retain the transverse coupling, but transform it by employing a Schrieffer-Wolff transformation, $U_S = \exp\left(iS\right)$, with generator $S = (g/\Delta E)\cos\zeta\left(a + a^\dagger\right)\sigma_y$, into a second-order longitudinal coupling. On the other hand, since $\hbar\omega_d \sim \Delta E$, we can drop within RWA the longitudinal driving term $-\hbar\Omega_{R0}\cos\left(\omega_d t\right)\sin\zeta\,\sigma_z$. The Hamiltonian then reads

$$
\begin{aligned}
H \;=\; & -\frac{1}{2}\,\Delta E\,\sigma_z + \hbar\Omega_{R0}\cos\left(\omega_d t\right)\cos\zeta\,\sigma_x + \hbar\omega_T\,a^\dagger a \\
& + g\sin\zeta\,\sigma_z\left(a + a^\dagger\right) - \frac{g^2}{\Delta E}\cos^2\zeta\,\sigma_z\left(a + a^\dagger\right)^2\;.
\end{aligned} \tag{3}
$$

A further unitary transformation with $U_R = \exp\left(-i\omega_d\sigma_z t/2\right)$ brings the Hamiltonian to the rotating frame, $\tilde{H} \equiv U_R H U_R^\dagger + i\hbar \dot{U}_R U_R^\dagger$. We obtain

$$\tilde{H} = \frac{1}{2}\hbar\delta\omega\,\sigma_z + \frac{1}{2}\hbar\Omega_{R0}\,\cos\zeta\,\sigma_x + \hbar\omega_T\,a^\dagger a$$
$$+ \ g\sin\zeta\,\sigma_z\left(a+a^\dagger\right) - \frac{g^2}{\Delta E}\cos^2\zeta\,\sigma_z\left(a+a^\dagger\right)^2.$$
$$(4)$$

Here $\delta\omega \equiv \omega_d - \Delta E/\hbar$ is the detuning. After diagonalization of the qubit terms we obtain

$$\tilde{H} = \frac{1}{2}\hbar\Omega_R\,\sigma_z + \hbar\omega_T\,a^\dagger a$$
$$+ \ g\sin\zeta\left[\sin\beta\,\sigma_z - \cos\beta\,\sigma_x\right]\left(a+a^\dagger\right)$$
$$- \ \frac{g^2}{\Delta E}\cos^2\zeta\left[\sin\beta\,\sigma_z - \cos\beta\,\sigma_x\right]\left(a+a^\dagger\right)^2. \quad (5)$$

Here $\Omega_R = \sqrt{\Omega_{R0}^2\cos^2\zeta + \delta\omega^2}$ and $\tan\beta = \delta\omega/(\Omega_{R0}\cos\zeta)$.

Finally we employ a second RWA. While the first one dropped terms oscillating with frequencies of order $\Delta E/\hbar$, the second one assumes the Rabi frequency Ω_R and the oscillator frequency ω_T to be fast. In the interaction representation with respect to the non-interacting Hamiltonian, $\tilde{H}_0 = (\hbar\Omega_R/2)\sigma_z + \hbar\omega_T\,a^\dagger a$, we then obtain

$$\tilde{H}_I = g_1\left(a^\dagger\sigma_-e^{-i(\Omega_R-\omega_T)t} + h.c.\right)$$
$$+ \ g_2\left(a^{\dagger 2}\sigma_-e^{-i(\Omega_R-2\omega_T)t} + h.c.\right)$$
$$+ \ g_3\left(a^\dagger a + aa^\dagger\right)\sigma_z. \quad (6)$$

We kept both single-photon and two-photon interactions with $g_1 = g\sin\zeta\cos\beta$ and $g_2 = (g^2/\Delta E)\cos^2\zeta\cos\beta$, although within RWA only one of them survives: the single-photon term for $\Omega_R \sim \omega_T$, or the two-photon term for $\Omega_R \sim 2\omega_T$. The last term of (6) with $g_3 = -(g^2/\Delta E)\cos^2\zeta\sin\beta$ is the ac-Stark effect, causing a qubit state dependent frequency shift of the oscillator [39]. In what follows we will assume that the qubit is kept near the symmetry point, i.e., $\epsilon \ll \Delta$ and $\cos\zeta \simeq 1$.

Transition rates in the rotation frame

The transformation to "dressed states" in the rotating frame modifies the relaxation, excitation and decoherence rates as compared to the standard results. To illustrate these effects and justify the treatment of the dissipation in latter sections we first consider a driven qubit (ignoring the coupling to the oscillator) coupled to a bath observable $\hat{X}_B$,

$$H = -\frac{1}{2}\Delta E\,\sigma_z + \hbar\Omega_{R0}\,\cos\left(\omega_d t\right)\sigma_x$$
$$- \ \frac{1}{2}\left(b_x\sigma_x + b_y\sigma_y + b_z\sigma_z\right)\hat{X}_B + H_{\text{bath}}. \quad (7)$$

In the absence of driving, $\Omega_{R0} = 0$, and for regular power spectra of the fluctuating bath observables we can proceed using Golden rule type arguments. The transverse noise is responsible for the relaxation and excitation with rates

$$\Gamma_\downarrow = \frac{|b_\perp|^2}{4\hbar^2}\langle\hat{X}_B^2(\omega = \Delta E)\rangle$$
$$\Gamma_\uparrow = \frac{|b_\perp|^2}{4\hbar^2}\langle\hat{X}_B^2(\omega = -\Delta E)\rangle, \quad (8)$$

while longitudinal noise produces a pure dephasing with rate [40]

$$\Gamma_\varphi^* = \frac{|b_z|^2}{2\hbar^2}S_X(\omega = 0). \quad (9)$$

Here $b_\perp \equiv b_x + ib_y$, and we introduced the ordered correlation function $\langle\hat{X}_B^2(\omega)\rangle \equiv \int dt\, e^{i\omega t}\langle\hat{X}_B(t)\hat{X}_B(0)\rangle$, as well as the power spectrum, i.e., the symmetrized correlation function, $S_X(\omega) \equiv (\langle\hat{X}_B^2(\omega)\rangle + \langle\hat{X}_B^2(-\omega)\rangle)/2$. The rates (8) and (9) also define the relaxation rate $1/T_1 = \Gamma_1 = \Gamma_\downarrow + \Gamma_\uparrow$ and the total dephasing rate $1/T_2 = \Gamma_\varphi = \Gamma_1/2 + \Gamma_\varphi^*$ which appear in the Bloch equations.

To account for the driving with frequency ω_d it is convenient to transform to the rotating frame via a unitary transformation $U_R = \exp\left(-i\omega_d\sigma_z t/2\right)$. Within RWA the transformed Hamiltonian reduces to

$$\tilde{H} = \frac{1}{2}\hbar\left[\Omega_{R0}\sigma_x + \delta\omega\sigma_z\right] \quad (10)$$
$$- \ \frac{1}{2}\left[b_z\sigma_z + b_\perp e^{i\omega_d t}\sigma_- + b_\perp^* e^{-i\omega_d t}\sigma_+\right]\hat{X}_B + H_{\text{bath}},$$

where $b_\perp \equiv b_x + ib_y$, and the detuning is $\delta\omega \equiv \omega_d - \Delta E/\hbar$. The RWA cannot be used in the second line of (10) since the fluctuations $\hat{X}_B$ contain potentially all frequencies, including those of order $\pm\omega_d$ which can compensate fast oscillations.

Diagonalizing the first line of (10) one obtains

$$\tilde{H} = \frac{1}{2}\hbar\Omega_R\,\sigma_z + H_{\text{bath}}$$
$$- \left[\frac{\sin\beta}{2}b_z + \frac{\cos\beta}{4}\left(b_\perp^* e^{-i\omega_d t} + b_\perp e^{i\omega_d t}\right)\right]\sigma_z\hat{X}_B$$
$$- \Bigg\{\left[\frac{(\sin\beta+1)}{4}b_\perp^* e^{-i\omega_d t} + \frac{(\sin\beta-1)}{4}b_\perp e^{i\omega_d t}\right.$$
$$\left. - \ \frac{\cos\beta}{2}b_z\right]\sigma_+\hat{X}_B + h.c.\Bigg\}, \quad (11)$$

with $\Omega_R = \sqrt{\Omega_{R0}^2 + \delta\omega^2}$ and $\tan\beta = \delta\omega/\Omega_{R0}$.

From here Golden-rule arguments yield the relaxation and excitation rates in the rotating frame [40]

$$\tilde{\Gamma}_\downarrow \approx \frac{b_z^2\cos^2\beta}{4\hbar^2}\langle\hat{X}_B^2(\omega = \Omega_R)\rangle \quad (12)$$
$$+ \ \frac{|b_\perp|^2}{16\hbar^2}(1-\sin\beta)^2\langle\hat{X}_B^2(\omega = \omega_d + \Omega_R)\rangle$$
$$+ \ \frac{|b_\perp|^2}{16\hbar^2}(1+\sin\beta)^2\langle\hat{X}_B^2(\omega = -\omega_d + \Omega_R)\rangle$$

and

$$\tilde{\Gamma}_\uparrow \approx \frac{b_z^2 \cos^2 \beta}{4\hbar^2} \langle \hat{X}_B^2(\omega = -\Omega_R)\rangle \tag{13}$$
$$+ \frac{|b_\perp|^2}{16\hbar^2}(1 - \sin\beta)^2 \langle \hat{X}_B^2(\omega = -\omega_d - \Omega_R)\rangle$$
$$+ \frac{|b_\perp|^2}{16\hbar^2}(1 + \sin\beta)^2 \langle \hat{X}_B^2(\omega = \omega_d - \Omega_R)\rangle ,$$

as well as the "pure" dephasing rate

$$\tilde{\Gamma}_\varphi^* \approx \frac{b_z^2 \sin^2 \beta}{2\hbar^2} S_X(\omega = 0) + \frac{\cos^2 \beta}{4\hbar^2}|b_\perp|^2 S_X(\omega = \omega_d) . \tag{14}$$

We note the effect of the frequency mixing, and due to the diagonalization the effects of longitudinal and transverse noise on relaxation and decoherence get mixed. In addition we note that the rates also depend on the fluctuations' power spectrum at the Rabi frequency.

For a sufficiently regular power spectrum of fluctuations with $\omega \approx \pm \Delta E/\hbar$, we can ignore the effect of detuning and the small shifts by $\pm\Omega_R$ as compared to the high frequency $\omega_d \approx \Delta E/\hbar$. We further assume that $\Omega_R \ll k_B T/\hbar$. In this case we find the simple relations

$$\tilde{\Gamma}_\uparrow = \frac{(1 + \sin\beta)^2}{4}\Gamma_\downarrow + \frac{(1 - \sin\beta)^2}{4}\Gamma_\uparrow + \frac{1}{2}\cos^2\beta\,\Gamma_\nu ,$$
$$\tilde{\Gamma}_\downarrow = \frac{(1 - \sin\beta)^2}{4}\Gamma_\downarrow + \frac{(1 + \sin\beta)^2}{4}\Gamma_\uparrow + \frac{1}{2}\cos^2\beta\,\Gamma_\nu ,$$
$$\tilde{\Gamma}_\varphi^* = \sin^2\beta\,\Gamma_\varphi^* + \frac{\cos^2\beta}{2}(\Gamma_\downarrow + \Gamma_\uparrow) , \tag{15}$$

where the rates in the lab frame are given by Eq. (8) and the new rate, $\Gamma_\nu \equiv \frac{1}{2}b_z^2 S_X(\Omega_R)$, depends on the power spectrum at the Rabi frequency.

To proceed we concentrate on the regime relevant for our system. Near the symmetry point of the qubit we have $b_z \approx 0$. At low temperatures, $k_B T \ll \Delta E \approx \hbar\omega_d$, we can neglect $\Gamma_\uparrow$ as it is exponentially small. Thus we are left with

$$\tilde{\Gamma}_{\downarrow/\uparrow} \approx \frac{(1 \mp \sin\beta)^2}{4}\Gamma_0 \quad , \quad \tilde{\Gamma}_\varphi^* \approx \frac{\cos^2\beta}{2}\Gamma_0 , \tag{16}$$

where

$$\Gamma_0 \equiv \frac{|b_\perp|^2}{4\hbar^2}\langle \hat{X}_B^2(\omega = \Delta E/\hbar)\rangle \approx \Gamma_\downarrow . \tag{17}$$

The ratio of up- and down-transitions depends on the detuning and can be expressed by an effective temperature. Right on resonance, where $\beta = 0$, we have $\tilde{\Gamma}_\uparrow = \tilde{\Gamma}_\downarrow$, corresponding to infinite temperature or a classical drive. For "blue" detuning, $\beta > 0$, we find $\tilde{\Gamma}_\uparrow > \tilde{\Gamma}_\downarrow$, i.e., *negative temperature*. This leads to a population inversion of the qubit, which is the basis for the lasing behavior which will be described below.
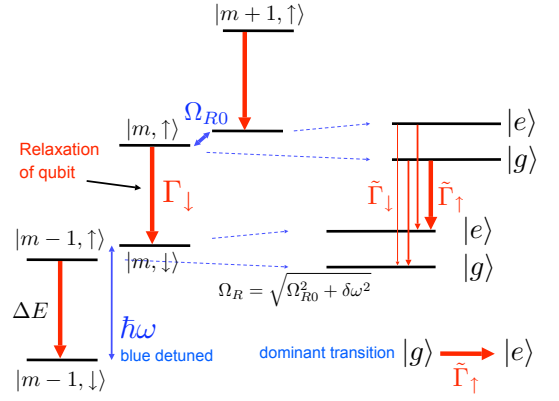

FIG. 2: Dressed states of a driven qubit near resonance. Here m is the number of photons of the driving field, which is assumed to be quantized.

In a more careful analysis, not making use of the "white noise" approximation, we obtain for $\beta = 0$

$$\frac{\tilde{\Gamma}_\downarrow}{\tilde{\Gamma}_\uparrow} = \frac{\langle \hat{X}_B^2(\omega = \omega_d + \Omega_R)\rangle}{\langle \hat{X}_B^2(\omega = \omega_d - \Omega_R)\rangle} . \tag{18}$$

For instance, for Ohmic noise and low bath temperature this reduces to $\tilde{\Gamma}_\downarrow/\tilde{\Gamma}_\uparrow \sim 1 + 2\Omega_R/\omega_d$. This corresponds to an effective temperature of order $2\hbar\omega_d/k_B \sim 2\Delta E/k_B$, which by assumption is high but finite. The infinite temperature threshold is crossed toward negative temperatures at weak blue detuning when the condition

$$\frac{(1 + \sin\beta)^2}{(1 - \sin\beta)^2} \sim 1 + \frac{2\Omega_R}{\omega_d} \tag{19}$$

is satisfied.

To illustrate how the population inversion is created for blue detuning we show in Fig. 2 the level structure, i.e., the formation of dressed states, of a near-resonantly driven qubit. For the purpose of this explanation the driving field is quantized. This level structure was described first by Mollow [26]. The picture also illustrates how for blue detuning a pure relaxation process, $\Gamma_\downarrow = \Gamma_0$, in the laboratory frame predominantly leads to an excitation process, $\tilde{\Gamma}_\uparrow$, in the rotating frame.

The Liouville equation in the rotating frame

Within the approximation leading to the rates (15) the Liouville equation governing the dynamics of the density matrix in the rotating frame can presented in a simple Lindblad form. Start in the lab frame the dissipation is accounted for by two damping terms,

$$\dot\rho = -\frac{i}{\hbar}[H, \rho] + L_Q\,\rho + L_R\,\rho . \tag{20}$$

The qubit's dissipation is described by

$$L_Q\rho = \frac{\Gamma_\downarrow}{2}\left(2\sigma_-\rho\sigma_+ - \rho\sigma_+\sigma_- - \sigma_+\sigma_-\rho\right)$$
$$+ \frac{\Gamma_\uparrow}{2}\left(2\sigma_+\rho\sigma_- - \rho\sigma_-\sigma_+ - \sigma_-\sigma_+\rho\right)$$
$$+ \frac{\Gamma_\varphi^*}{2}\left(\sigma_z\rho\sigma_z - \rho\right) , \qquad (21)$$

with rates given by (8) and (9). The resonator damping, with strength parametrized by κ, can be written as [41]

$$L_R\rho = \frac{\kappa}{2}\left(N_{\text{th}} + 1\right)\left(2a\rho a^\dagger - a^\dagger a\rho - \rho a^\dagger a\right)$$
$$+ \frac{\kappa}{2}N_{\text{th}}\left(2a^\dagger\rho a - aa^\dagger\rho - \rho aa^\dagger\right) . \qquad (22)$$

Here $N_{\text{th}} = 1/\left[\exp(\hbar\omega_T/k_B T) - 1\right]$ is the thermal distribution function of photons in the resonator.

The transformations to the rotating frame and RWA described above transform the Liouville equation to a new form, which in our approximation again has a Lindblad form. In the interaction representation it is

$$\dot{\tilde{\rho}} = -\frac{i}{\hbar}\left[\tilde{H}_I, \tilde{\rho}\right] + \tilde{L}_Q\,\tilde{\rho} + L_R\,\tilde{\rho} , \qquad (23)$$

where

$$\tilde{L}_Q\tilde{\rho} = \frac{\tilde{\Gamma}_\downarrow}{2}\left(2\sigma_-\tilde{\rho}\sigma_+ - \tilde{\rho}\sigma_+\sigma_- - \sigma_+\sigma_-\tilde{\rho}\right)$$
$$+ \frac{\tilde{\Gamma}_\uparrow}{2}\left(2\sigma_+\tilde{\rho}\sigma_- - \tilde{\rho}\sigma_-\sigma_+ - \sigma_-\sigma_+\tilde{\rho}\right)$$
$$+ \frac{\tilde{\Gamma}_\varphi^*}{2}\left(\sigma_z\tilde{\rho}\sigma_z - \tilde{\rho}\right) , \qquad (24)$$

while the oscillator damping term is not affected by the transformation. Although at low temperatures in the lab frame the relaxation processes dominate (see Eq. 17), the transformation to the rotating frame introduces excitation and pure dephasing processes.

THE SINGLE-QUBIT LASER

In the following we will consider two resonance situations, $\Omega_R \sim \omega_T$ or $\Omega_R \sim 2\omega_T$, when either the one- or the two-photon interactions dominate, and investigate the effects of blue or red detuning, $\delta\omega \equiv \omega_d - \Delta E/\hbar$, of the qubit driving frequency. We also study the effects of detuning of the Rabi frequency Ω_R relative to that of the oscillator.

One-photon interaction

When the Rabi frequency is in resonance with the oscillator, $\Omega_R \approx \omega_T$, the Hamiltonian (6) in RWA reduces to

$$H_I = g_1\left(a^\dagger\sigma_- e^{-i(\Omega_R - \omega_T)t} + h.c.\right)$$
$$+ g_3\left(a^\dagger a + aa^\dagger\right)\sigma_z . \qquad (25)$$

From here we can proceed in the frame of the standard semiclassical approach [41, 42] of laser physics with the following main steps: In the absences of fluctuations the system is described by Maxwell-Bloch equations for the classical variables $\alpha = \langle a\rangle$, $\alpha^* = \langle a^\dagger\rangle$, $s_\pm = \langle\sigma_\pm\rangle$ and $s_z = \langle\sigma_z\rangle$, which can be derived from the Hamiltonian (25) if all correlation functions are assumed to factorize. Next the qubit variables can be adiabatically eliminated as long as $\kappa, g_1 \ll \tilde{\Gamma}_1, \tilde{\Gamma}_\varphi$, which leads to a closed equation of motion for α. If we finally account for fluctuations, e.g., due to thermal noise in the resonator, α becomes a stochastic variable obeying a Langevin equation [41],

$$\dot{\alpha} = -\left[\kappa - \frac{C}{\tilde{\Gamma}_\varphi + i\delta\Omega}s_z^{st} + 4ig_3 s_z^{st}\right]\frac{\alpha}{2} + \xi(t). \qquad (26)$$

Here $C \equiv 2g_1^2$, $s_z^{st} = -D_0/\left(1 + |\alpha|^2/\tilde{n}_0\right)$ is the stationary value of the population difference between the qubit levels, and $D_0 = \left(\tilde{\Gamma}_\downarrow - \tilde{\Gamma}_\uparrow\right)/\tilde{\Gamma}_1$ is the normalized difference between the rates with $\tilde{\Gamma}_1 = \tilde{\Gamma}_\uparrow + \tilde{\Gamma}_\downarrow$. We further introduced the photon saturation number $n_0 = \tilde{\Gamma}_\varphi\tilde{\Gamma}_1/4g_1^2$ and $\tilde{n}_0 \equiv n_0(1 + \delta\Omega^2/\tilde{\Gamma}_\varphi^2)$, and the total dephasing rate $\tilde{\Gamma}_\varphi = \tilde{\Gamma}_1/2 + \tilde{\Gamma}_\varphi^*$. The detuning of the Rabi frequency enters in combination with a frequency renormalization, $\delta\Omega \equiv \Omega_R - \omega_T + g_3|\alpha|^2$. The Langevin force due to thermal noise in the oscillator satisfies $\langle\xi(t)\xi^*(t')\rangle = \kappa N_{\text{th}}\delta(t - t')$ and $\langle\xi(t)\xi(t')\rangle = 0$. Noise originating from the qubit can be neglected provided the thermal noise is strong, $\kappa N_{\text{th}} \gg g_1^2/\tilde{\Gamma}_\varphi$.

Two-photon interaction

The two-photon effect dominates near the resonance condition $\Omega_R \approx 2\omega_T$. In RWA the Hamiltonian reduces to

$$H_I = g_2\left(a^{\dagger 2}\sigma_- e^{-i(\Omega_R - 2\omega_T)t} + h.c.\right)$$
$$+ g_3\left(a^\dagger a + aa^\dagger\right)\sigma_z . \qquad (27)$$

The corresponding Langevin equation for the resonator variable reads

$$\dot{\alpha} = -\left[\kappa - \frac{C}{\tilde{\Gamma}_\varphi + i\delta\Omega}s_z^{st} + 4ig_3 s_z^{st}\right]\frac{\alpha}{2} + \xi(t), \qquad (28)$$

i.e., is of the same form as Eq. (26) but with $C \equiv 4g_2^2|\alpha|^2$ and $s_z^{st} = -D_0/\left(1 + (|\alpha^2|/\tilde{n}_0)^2\right)$. The photon saturation number is now given by $n_0 = (\tilde{\Gamma}_\varphi\tilde{\Gamma}_1/4g_2^2)^{1/2}$, and $\tilde{n}_0 \equiv n_0(1 + \delta\Omega^2/\tilde{\Gamma}_\varphi^2)^{1/2}$. Again $\xi(t)$ represents thermal noise,
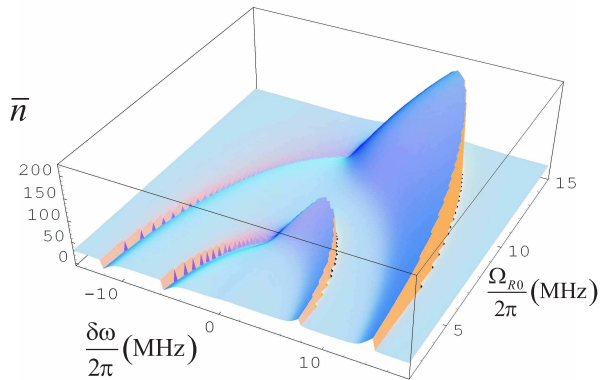
FIG. 3: Average number of photons in the resonator as function of the driving detuning $\delta\omega$ and amplitude Ω_{R0}. Peaks at $\delta\omega > 0$ correspond to lasing, while dips at $\delta\omega < 0$ correspond to cooling. The inner curve corresponds to the one-photon resonance which exists only away from the symmetry point. Here we assumed $\epsilon = 0.01\Delta$. The outer curve describes the two-photon resonance, which persists at $\epsilon = 0$. In domains of bistability the lowest value of $\bar{n}$ is plotted (leading to the sharp drops in both curves). We chose the following parameters for the qubit: $\Delta/2\pi = 1$ GHz, $\epsilon = 0.01\Delta$, $\Gamma_0/2\pi = 125$ kHz, the resonator: $\omega_T/2\pi = 6$MHz, $\kappa/2\pi = 0.34$ kHz, and the coupling: $g/2\pi = 3.3$ MHz. The bath temperature is $T = 10$ mK.

while noise arising from the qubit can be neglected if $\kappa N_{\text{th}} \gg g_2^2 \bar{n}/\tilde{\Gamma}_\varphi$. The detuning of the Rabi frequency for two-photon interaction is given by $\delta\Omega \equiv \Omega_R - 2\omega_T + g_3|\alpha|^2$.

Results obtained from the Langevin equation

If one neglects the frequency shifts of the oscillator, i.e., for $g_3 = 0$, the Fokker-Planck equations corresponding to the Langevin equations (26) and (28) have exact analytic solutions [42]. Also for $g_3 \neq 0$ the Eqs. (26) and (28) written as $\dot{\alpha} = -f(n)\alpha/2 + \xi(t)$ can be transformed to equations for the average number of photons $\langle|\alpha|^2\rangle = \bar{n}$ in the form $\dot{\bar{n}} = -\langle n\text{Re}[f(n)]\rangle + \kappa N_{\text{th}}$. In the steady state, for $\bar{n} \gg 1$ they can be approximated by $\bar{n}\text{Re}[f(\bar{n})] = \kappa N_{\text{th}}$. The results of this analysis are shown in Fig. 3. To demonstrate both the one-photon and the two-photon effects we have assumed a small deviation from the symmetry point, $\epsilon = 0.01\Delta$. The two-photon resonance (the outer one) persist even for $\epsilon = 0$, while the one-photon resonance (the inner one) vanishes there. We observe that the solution shows bistability bifurcations (see below). As a result we see in in Fig. 3 sharp drops of $\bar{n}$ for both resonances as only the lowest stable value is plotted .

We can estimate the asymptotic solutions analytically. In the one-photon case, assuming $\bar{n} \gg \tilde{n}_0$, we obtain
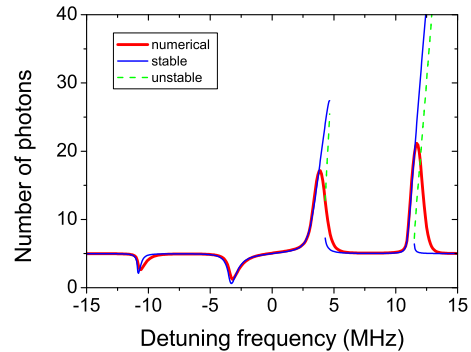

FIG. 4: Average number of photons $\bar{n}$ versus the detuning. The blue curves are obtained from the Langevin equations (26) and (28). They show the bistability with the solid curve denoting stable solutions, while the dashed curve denotes the unstable solution. The red curve is obtained from a numerical solution of the master equation (23). The driving amplitude is taken as $\Omega_{R0}/2\pi = 5$MHz. The parameters of the qubit: $\Delta/2\pi = 1$ GHz, $\epsilon = 0.01\Delta$, $\Gamma_0/2\pi = 125$ kHz, the resonator: $\omega_T/2\pi = 6$MHz, $\kappa/2\pi = 1.7$ kHz, $N_{\text{th}} = 5$, and the coupling: $g/2\pi = 3.3$ MHz.

from Eq.(26)

$$\bar{n} \sim N_{\text{th}} + \frac{(-D_0)\tilde{\Gamma}_1}{2\kappa} . \tag{29}$$

This result holds independent of whether the second contribution due to the qubit is larger or smaller than the thermal number N_{th} as long as $\bar{n} \gg \tilde{n}_0$. In the two-photon case, assuming $\bar{n} \gg \tilde{n}_0$, we obtain from Eq.(28)

$$\bar{n} \sim N_{\text{th}} + \frac{(-D_0)\tilde{\Gamma}_1}{\kappa} . \tag{30}$$

Solution of the master equation

We also solved the full master equation (23) numerically, which provides access not only to the average number of photons in the oscillator, $\bar{n}$, but also to the whole distribution function $P(n)$. To reach convergence with a limited number of photon basis states ($n \leq 100$) we assumed a low thermal number, $N_{\text{th}} = 5$ and a relatively high relaxation constant of the oscillator $\kappa/2\pi = 1.7$ kHz. In Fig. 4 the solutions of the Langevin equations (26) and (28) and those of the master equation (23) is compared.

In Fig. 5 the Fano factor $F = (\langle n^2 \rangle - \langle n \rangle^2)/\langle n \rangle$ of the photon number distribution is presented. We observe two phenomena. First, in the regime of the lasing without bistability the Fano factor is reduced as compared to that of the thermal state. In the bistable regime it is increased due to the switching between the two solutions.

In Fig. 6 the distribution function, $P(n)$, for the number of photons in the oscillator is plotted both for the
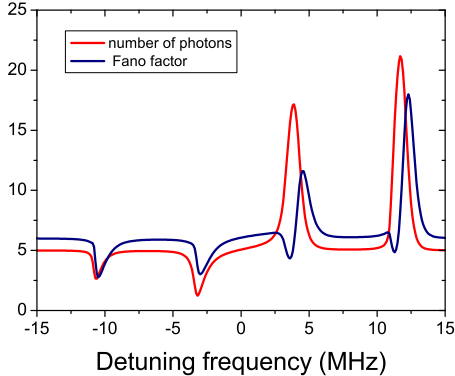
FIG. 5: The Fano factor (blue), and the average photon number $\bar{n}$ (red). The parameters are as in Fig. 4.
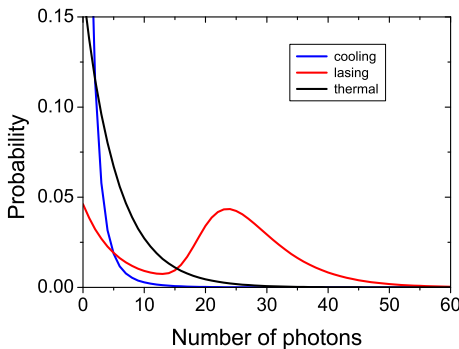

FIG. 6: The distribution function, $P(n)$, obtained by numerically solving the master equation (23). Blue curve: cooling regime of the one-photon resonance with $\Omega_{R0} = 2\pi \times 5\text{MHz}$ and $\delta\omega = -2\pi \times 3.2\text{MHz}$. Red curve: lasing regime of the two-photon resonance with $\Omega_{R0} = 2\pi \times 5\text{MHz}$ $\delta\omega = 2\pi \times 11.7\text{MHz}$. We observe a peak in the $P(n)$ distribution between $n = 20$ and 30 as a result of the lasing behavior. Black curve: thermal distribution with $N_{\text{th}} = 5$. The parameters are as in Fig. 4.

cooling and enhancement regime. For comparison also the thermal (Bose-Einstein) distribution is plotted.

The enhancement and cooling effects described here rely crucially on the transition rates, i.e., the dissipative effects as described by the Liouville equations. In order to demonstrate this dependence we show in Fig. 7 the dependence of the average photon number on the qubit's relaxation rate at the one-photon resonance. We note a non-monotonic dependence on the qubit's relaxation rate. Above the saturation threshold for $\bar{n} > n_0$ the pumping rate is limited by Γ_0, leading to a roughly linear growth of the photon number with increasing Γ_0, consistent with Eq. (29). At the saturation threshold for $\bar{n} \sim n_0$ the effective coupling is determined by g_1 and the photon number becomes insensitive to small variations of
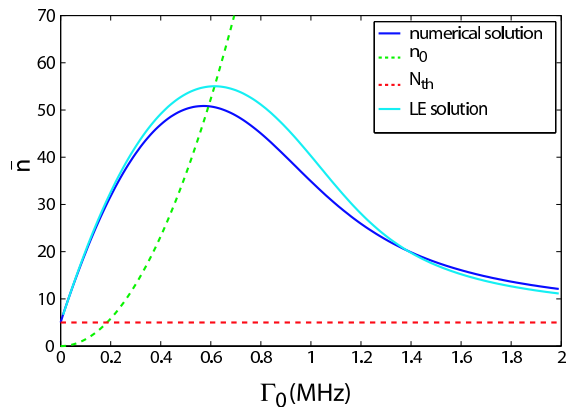

FIG. 7: Average number of photons in the resonator as function of the qubit's relaxation rate, Γ_0 at the one-photon resonance, $\Omega_R = \omega_T$ for $g_3 = 0$ and $N_{\text{th}} = 5$. The dark blue line shows the numerical solution of the master equation, the light blue solid line represents the solution of the Langevin equation, Eq. (26). The green and red dashed curves represent respectively the saturation number n_0 and the thermal photon number N_{th}. The parameters are as in Fig. 4 (except for Γ_0).

Γ_0. Finally, for $\bar{n} < n_0$, an increase of Γ_0 predominantly increases the dephasing rate $\tilde{\Gamma}_\varphi$. As can be seen from Eq. (26) this destroys the coherent coupling between qubit and oscillator and the photon number decreases towards N_{th}. In Figure 7 we plot both the results of a numerical solution of the master equation and the Langevin approximation. We find good agreement between both (except for the bistability in the corresponding parameter regions).

RESULTS AND DISCUSSION

We summarize our main conclusions. Our results for the number of photons $\bar{n}$ are plotted in Fig. 3 as a function of the detuning $\delta\omega$ of the driving frequency and driving amplitude Ω_{R0}. It exhibits sharp structures along two curves corresponding to the one- and two-photon resonance conditions, $\Omega_R = \omega_T - g_3\bar{n}$ and $\Omega_R = 2\omega_T - g_3\bar{n}$. Blue detuning, $\delta\omega > 0$, induces a strong population inversion of the qubit levels, which in resonance leads to one-qubit lasing. In experiments the effect can be measured as a strong increase of the number of photons in the resonator above the thermal values. Red detuning produces a one-qubit cooler with resulting photon numbers substantially below the thermal value.

The bistability of the solution of the Langevin description is illustrated in Fig. 4. In the range of bistability we expect a telegraph-like noise corresponding to the random switches between the two solutions.

Potentially useful applications of the considered scheme are the lasing behavior and the creation of a highly non-thermal population of the oscillator as well as

the cooling. Within the accuracy of our approach we estimate that a population of order $\bar{n} = 1$ can be reached for optimal detuning. A more detailed analysis is required to determine the precise cooling limit.

So far we described an LC oscillator coupled to a flux qubit. But our analysis equally applies for a nano-mechanical resonator coupled capacitively to a Josephson charge qubit (see Fig. 1b). In this case σ_z stands for the charge of the qubit and both the coupling to the oscillator as well as the driving are capacitive, i.e., involve σ_z. To produce the capacitive coupling between the qubit and the oscillator, the latter could be metal-coated and charged by the voltage source V_x. The dc component of the gate voltage V_g puts the system near the charge degeneracy point where the dephasing due to the $1/f$ charge noise is minimal. Rabi driving is induced by an *ac* component of V_g. Realistic experimental parameters are expected to be very similar to the ones used in the examples discussed above, except that a much higher quality factor of the resonator ($\sim 10^5$) and a much higher number of quanta in the oscillator can be reached. This number will easily exceed the thermal one, thus a proper lasing state with Poisson statistics, appropriately named SASER [28], is produced. One should then observe the usual line narrowing with line width given by $\kappa N_{\text{th}}/(4\bar{n}) \sim \kappa^2 N_{\text{th}}/\tilde{\Gamma}_1$. Experimental observation of this line-width narrowing would constitute a confirmation of the lasing/sasing.

ACKNOWLEDGMENT

[1] E. Il'ichev, N. Oukhanski, A. Izmalkov, Th. Wagner, M. Grajcar, H.-G. Meyer, A. Yu. Smirnov, Alec Maassen van den Brink, M. H. S. Amin, and A. M. Zagoskin. Continuous monitoring of Rabi oscillations in a Josephson flux qubit. *Phys. Rev. Lett.*, 91:097906, 2003.

[2] A. Wallraff, D. I. Schuster, A. Blais, L. Frunzio, R.-S. Huang, J. Majer, S. Kumar, S. M. Girvin, and R. J. Schoelkopf. Circuit quantum electrodynamics: Coherent coupling of a single photon to a Cooper pair box. *Nature*, 431:162, 2004.

[3] I. Chiorescu, P. Bertet, K. Semba, Y. Nakamura, C. J. P. M. Harmans, and J. E. Mooij. Coherent dynamics of a flux qubit coupled to a harmonic oscillator. *Nature*, 431:159, 2004.

[4] A. Wallraff, D. I. Schuster, A. Blais, L. Frunzio, J. Majer, M. H. Devoret, S. M. Girvin, and R. J. Schoelkopf. Approaching unit visibility for control of a supercon-ducting qubit with dispersive readout. *Phys. Rev. Lett.*, 95:060501, 2005.

[5] J. Johansson, S. Saito, T. Meno, H. Nakano, M. Ueda, K. Semba, and H. Takayanagi. Vacuum Rabi oscillations in a macroscopic superconducting qubit LC oscillator system. *Phys. Rev. Lett.*, 96(12):127006, Mar 2006.

[6] A. Naik, O. Buu, M. D. LaHaye, A. D. Armour, A. A. Clerk, M. P. Blencowe, and K. C. Schwab. Cooling a nanomechanical resonator with quantum back-action. *Nature*, 443:193, 2006.

[7] M. Grajcar, S. H. W. van der Ploeg, A. Izmalkov, E. Il'ichev, H. G. Meyer, A. Fedorov, A. Shnirman, and G. Schön. Sisyphus damping and amplification by a superconducting qubit. *arXiv.org:0708.0665*, 2007.

[8] F. Deppe, M. Mariantoni, E. P. Menzel, A. Marx, S. Saito, K. Kakuyanagi, H. Tanaka, T. Meno, K. Semba, H. Takayanagi, E. Solano, and R. Gross. Two-photon probe of the Jaynes-Cummings model and symmetry breaking in circuit QED. *arXiv.org:0805.3294*, 2008.

[9] O. Buisson, F. Balestro, J. P. Pekola, and F. W. J. Hekking. One-shot quantum measurement using a hysteretic dc SQUID. *Phys. Rev. Lett.*, 90:238304, 2003.

[10] A. Blais, R. S. Huang, A. Wallraff, S. M. Girvin, and R. J. Schoelkopf. Cavity quantum electrodynamics for superconducting electrical circuits: an architecture for quantum computation. *Phys. Rev. A*, 69:062320, 2004.

[11] Yu-xi Liu, L. F. Wei, and F. Nori. Generation of non-classical photon states using a superconducting qubit in a microcavity. *Europhys. Lett.*, 67:941, 2004.

[12] I. Martin, A. Shnirman, L. Tian, and P. Zoller. Ground state cooling of mechanical resonators. *Phys. Rev. B*, 69:125339, 2004.

[13] K. Moon and S. M. Girvin. Theory of microwave parametric down-conversion and squeezing using circuit QED. *Phys. Rev. Lett.*, 95:140504, 2005.

[14] M. Mariantoni, M. J. Storcz, F. K. Wilhelm, W. D. Oliver, A. Emmert, A. Marx, R. Gross, H. Christ, and E. Solano. On-chip microwave fock states and quantum homodyne measurements. *cond-mat/0509737*, 2005.

[15] Yu-xi Liu, C. P. Sun, and F. Nori. Scalable superconducting qubit circuits using dressed states. *Phys. Rev. A*, 74:052321, 2006.

[16] M. Wallquist, V. S. Shumeiko, and G. Wendin. Selective coupling of superconducting qubits via tunable stripline cavity. *Phys. Rev. B*, 74:224506, 2006.

[17] Fei Xue, Y. D. Wang, C. P. Sun, H. Okamoto, H. Yamaguchi, and K. Semba. Controllable coupling between flux qubit and nanomechanical resonator by magnetic field. *New J. Phys.*, 9:35, 2007.

[18] J. Hauss, A. Fedorov, C. Hutter, A. Shnirman, and G. Schön. Single-qubit lasing and cooling at the Rabi frequency. *Phys. Rev. Lett.*, 100:037003, 2008.

[19] S. Ashhab, J. R. Johansson, A. M. Zagoskin, and F. Nori. Single-artificial-atom lasing and its suppression by strong pumping. *arXiv.org:0803.1209*, 2008.

[20] K. Jaehne, K. Hammerer, and M. Wallquist. Ground state cooling of a nanomechanical resonator via a Cooper pair box qubit. *arXiv.org:0804.0603*, 2008.

[21] A. Yu. Smirnov. Theory of weak continuous measurements in a strongly driven quantum bit. *Phys. Rev. B*, 68:134514, 2003.

[22] Ya. S. Greenberg, E. Il'ichev, and A. Izmalkov. Low frequency Rabi spectroscopy for a dissipative two-level system. *Europhys. Lett.*, 72:880, 2005.

[23] Yi Mu and C. M. Savage. One-atom lasers. *Phys. Rev. A*, 46(9):5944–5954, Nov 1992.

[24] J. McKeever, A. Boca, A. D. Boozer, J. R. Buck, and H. J. Kimble. Experimental realization of a one-atom laser in the regime of strong coupling. *Nature*, 425:268, 2003.

[25] J. Zakrzewski, M. Lewenstein, and T. W. Mossberg. Theory of dressed-state lasers. I. Effective Hamiltonians and stability properties. *Phys. Rev. A*, 44:7717, 1991.

[26] B. R. Mollow. Power spectrum of light scattered by two-level systems. *Phys. Rev.*, 188(5):1969–1975, Dec 1969.

[27] D. Jonathan and M. B. Plenio. Light-shift-induced quantum gates for ions in thermal motion. *Phys. Rev. Lett.*, 87(12):127901, Sep 2001.

[28] A. J. Kent, R. N. Kini, N. M. Stanton, M. Henini, B. A. Glavin, V. A. Kochelap, and T. L. Linnik. Acoustic phonon emission from a weakly coupled superlattice under vertical electron transport: Observation of phonon resonance. *Phys. Rev. Lett.*, 96:215504, 2006.

[29] T. A. Fulton, P. L. Gammel, D. J. Bishop, L. N. Dunkleberger, and G. J. Dolan. Observation of combined Josephson and charging effects in small tunnel junction circuits. *Phys. Rev. Lett.*, 63:1307, 1989.

[30] A. Maassen van den Brink, G. Schön, and L. J. Geerligs. Combined single electron and coherent Cooper pair tunneling in voltage-biased Josephson junctions. *Phys. Rev. Lett.*, 67:3030, 1991.

[31] A. Maassen van den Brink, A. A. Odintsov, P. A. Bobbert, and G. Schön. Coherent Cooper pair tunneling in systems of Josephson junctions: Effects of quasiparticle tunneling and of the electromagnetic environment. *Z. Physik B*, 85:459, 1991.

[32] Ya. M. Blanter, O. Usmani, and Yu. V. Nazarov. Single-electron tunneling with strong mechanical feedback. *Phys. Rev. Lett.*, 93:136802, 2004.

[33] M. P. Blencowe, J. Imbers, and A. D. Armour. Dynamics of a nanomechanical resonator coupled to a superconducting single-electron transistor. *New J. Phys.*, 7:236, 2005.

[34] A. A. Clerk and S. Bennett. Quantum nano-electromechanics with electrons, quasiparticles and Cooper pairs: effective bath descriptions and strong feedback effects. *New J. Phys.*, 7:238, 2005.

[35] S. D. Bennett and A. A. Clerk. Laser-like instabilities in quantum nano-electromechanical systems. *Phys. Rev. B*, 74:201301, 2006.

[36] O. Usmani, Ya. M. Blanter, and Yu. V. Nazarov. Strong feedback and current noise in nanoelectromechanical systems. *Phys. Rev. B*, 75(19):195312, 2007.

[37] D. A. Rodrigues, J. Imbers, and A. D. Armour. Quantum dynamics of a resonator driven by a superconducting single-electron transistor: A solid-state analogue of the micromaser. *Phys. Rev. Lett.*, 98(6):067204, 2007.

[38] O. Astafiev, K. Inomata, A. O. Niskanen, T. Yamamoto, Yu. A. Pashkin, Y. Nakamura, and J. S. Tsai. Single artificial-atom laser. *Nature*, 449:588–590, 2007.

[39] Ya. S. Greenberg, A. Izmalkov, M. Grajcar, E. Il'ichev, W. Krech, H.-G. Meyer, M. H. S. Amin, and A. Maassen van den Brink. Low-frequency characterization of quantum tunneling in flux qubits. *Phys. Rev. B*, 66:214525, 2002.

[40] G. Ithier, E. Collin, P. Joyez, P.J. Meeson, D. Vion, D. Esteve, F. Chiarello, A. Shnirman, Yu. Makhlin, J. Schriefl, and G. Schön. Decoherence in a superconducting quantum bit circuit. *Phys. Rev. B*, 72:134519, 2005.

[41] C. W. Gardiner and P. Zoller. *Quantum noise.* Springer, 3-d edition, 2004.

[42] M. Reid, K. J. McNeil, and D. F. Walls. Unified approach to multiphoton lasers and multiphoton bistability. *Phys. Rev. A*, 24:2029, 1981.